TECHNICAL RESEARCH REPORT

SYSTEMS RESEARCH CENTER

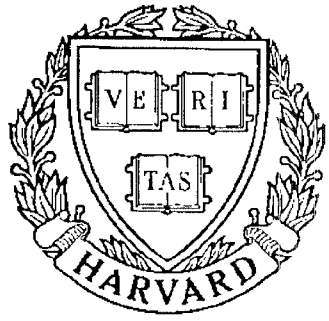

Supported by the National Science Foundation Engineering Research Center Program (NSFD CD 8803012), Industry and the University

Dynamic Generation of Machined Surfaces Part 1: Description of a Random Excitation System

by G.M. Zhang and S.G. Kapoor

TR 90-36

Dynamic Generation of Machined Surfaces
Part 1: Description of a Random Excitation System

G. M. Zhang, Assistant Professor
Mechanical Engineering Department and Systems Research Center
University of Maryland
College Park, MD 20742

S. G. Kapoor, Associate Professor
Department of Mechanical and Industrial Engineering
University of Illinois at Urbana-Champaign
Urbana, Illinois 61801

Abstract

With increasing emphasis on the adaptive control for the purpose of quality and productivity improvement, it becomes necessary to develop models which can correlate the surface finish parameters with the machining conditions as well as workpiece material characteristics. This paper presents a study that leads to the development of a model for the dynamic generation of three-dimensional texture of machined surfaces. In Part 1, the mathematical formulation of the random excitation system which is responsible for the random portion of a surface profile is developed. It is assumed that the random excitation system originates from the nonhomogeneous distribution of microhardness of workpiece material. Machining tests are also performed to verify the validity of such a model development. In Part 2, a procedure for the construction of three-dimensional topography will be developed and the relationship between the machining conditions and the surface finish parameters will be established.

1 Introduction

It is well known that the roughness profile of a cut surface contains periodic components [1-4]. The geometry of cutting action, namely, the tool geometry and cutting parameters are commonly presumed to be the main factors relating to the formation of the deterministic portion of the surface profile. Under ideal conditions, the roughness profile is formed by the repetition of the tool tip profile at intervals of feed (per revolution) and it is easy to correlate the roughness indices such as R_a and RMS values with the cutting parameters [5,6]. On the other hand, workpiece material properties, tool vibration, metal shearing during the

chip formation, etc., interact in a complex manner and their effects are dealt with as the random portion of roughness profile. Evaluation of the random or stochastic components of the surface profile still remains to be done. More recently, researchers have tried to establish quantitative relations between the surface finish and the cutting parameters of depth of cut, feed, and cutting speed using the methods like wavelength decomposition of surface roughness [7] and the constant-R_a contour map [8]. Unfortunately, no positive results on such quantitative relations have been reported and the randomness observed in any roughness profiles is explained qualitatively.

The purpose of these two-part papers is to develop a model which is capable of constructing the three-dimensional texture of machined surfaces with both deterministic and stochastic components in it. In this study, an assumption has been made that the stochastic or random components of a surface profile could come from the tool vibratory motion caused by the random excitation. This random excitation in turn originates from the force variation caused by the nonhomogeneous distribution of microhardness present in the workpiece material being machined [11].

In part 1, a mathematical model is developed to describe the phenomenon of random excitation. The model formulation is based on the sample variance theory [9,10], which relates the random excitation phenomenon to factors such as the microhardness, size, and shape of the microstructures present in the workpiece material, as well as the three cutting parameters, namely, the depth of cut, feed, and cutting speed. As a result, the developed mathematical model provides a means to quantitatively evaluate how the microstructures of the workpiece material and the three cutting parameters are related to the random tool motion. Cutting tests are also carried out to confirm the validity of the developed model. In part 2, a procedure will be developed to construct the surface topography using the results of the random excitation model and the geometric action of cutting tool. The implications of the present research are far reaching as it can benefit both the manufacturing engineers in generating surfaces with prescribed or desired characteristics related to part function and

the design engineers in specifying properties of workpiece materials and proper dimensional tolerances which can be achieved on the shop floor.

2 Random Excitation System

2.1 Excitation Source

Figure 1 presents a pictorial view of a possible excitation source which causes the random tool motion druing machining. Figure 1a is a micrograph of ferrite and pearlite structures present in mild carbon steel at room temperature [12]. Figure 1b indicates that the cutting edge experiences different microstructural portions during time intervals Δt_1 and Δt_2. Due to the fact that the pearlite structure is harder than the ferrite structure, the generated cutting force varies both dynamically and randomly. In the present work, a concept of random excitation system is introduced to model this mechanism which causes the tool to randomly vibrate. This random excitation system is directly related to (1) the existence of a nonhomogeneous microstructural distribution; and (2) the cutting process because it instantly feeds various microstructural portions to the cutting edge during machining, just like taking samples from the nonhomogeneous microstructural distribution. In fact, the sample size is determined by the three cutting parameters of depth of cut (d), feed (f), and cutting speed (v). The larger the three cutting parameter values, the larger the sample size.

2.2 Issues Related to the Random Excitation System

In the process of developing the random excitation system model, two issues need to be addressed. The first issue deals with the characteristics of microstructural distribution present in the material being cut. The second issue is related to the cutting process, or the sampling process, as explained in section 2.1.

The microhardness distribution involves important factors such as the hardness of individual microstructures or the microhardness, and the geometric shape and size of the microstructures. For example, if the difference of microhardness between two microstruc-

tures is significant, the cutting force variation induced by this hardness variation would also be significant. The microstructures having small sizes with spherical shapes tend to be homogeneous in any nature. On the other hand, the microstructures having large sizes with irregular shapes often display certain degrees of nonhomogeneity in the physical property of microhardness.

The sampling process involves important factors such as the sample volume (i.e., the sample size) and its geometric shape. The importance of sample volume in assessing the degree of nonhomogeneity is evident. For example, large sample volumes could average out the possible influence caused by the differences in the size and shape of the microstructures. On the other hand, too small a sample volume could result into a significant degree of nonhomogeneity regarding the microstructural contents within sample.

2.3 Sample Shape and Three Cutting Parameters

In order to further clarify the concept that the cutting process can be viewed as a sampling process in the model development of random excitation system, the relation between the geometric sample shape and the three cutting parameters of depth of cut, feed, and cutting speed for a single point cutting process is explained.

Figure 2 presents a boring machining process. The removed chip volume during one revolution of the workpiece can be thought of as a volumetric sum of a series of samples identical in geometric shape passing through the shear zone. The geometric shape of each sample shown in Fig. 2 is a parallelepiped. Its cross-sectional area is equal to a product of depth of cut and feed. As feed or/and depth of cut increase, the sample volume increases accordingly. In addition, for a large slenderness ratio, which is the ratio of depth of cut to feed [13], a narrow chip cross-section is created, leading to a narrow-shaped sample volume. This usually causes an increase of hardness variation among the samples, a phenomenon which will be explained later in this paper.

The parameter of cutting speed, or spindle speed for a given workpiece diameter D,

is related to the number of samples to be taken during one revolution of the workpiece. As illustrated in Fig. 2, one dimension of sample is given by $\pi D/n_s$ where parameter n_s represents the number of samples to be selected during one revolution of the workpiece. A large number of samples, or a large n_s, allows frequent drop-downs and jump-ups in the magnitude of the cutting force. The frequency of such down-ward to jump-up or jump-up to down-ward during one revolution of the workpiece is is given by $\frac{n_s}{2}$. Due to this fact, the highest frequency f_{max} in the cutting force variation which can be described by the random excitation model is given by

$$f_{max} = \frac{n_s}{2}\frac{N}{60} \tag{1}$$

where N =spindle speed, rpm.

3 Mathematical Formulation of the Random Excitation System

As discussed in the previous sections, the random tool motion is due to the presence of the nonhomogeneous distribution of microhardness. The cutting process, viewed as a sampling process, is directly related to the origination of the random excitation system. The three cutting parameters of depth of cut, feed and cutting speed determine the sample shape and size. The mathematical formulation of this random excitation system consists of the following three stages.

3.1 Nonhomogeneous Distribution of Microhardness

A statistical approach is proposed to formulate the nonhomogeneous distribution of microhardness. A representative part is chosen from the workpiece material. The microstructural constituents as well as their microhardness values are experimentally identified, say H_i for $i = 1, 2, \cdots, n$ where n represents the number of measurement locations on the chosen part. Based on these data, the three statistics, namely, mean μ_a, variance σ_a^2, and the correlation coefficient function $\rho(r)$, are calculated using the standard statistical formulas. Note that

parameter r of the correlation coefficient function represents the distance in space between ith and i'th measurement locations. These three statistics provide quantitative information on the size, the shape, and the segregation of microstructures and depict the microhardness distribution present in the material being machined. They also form a basis for quantifying the effect of the micro-constituent scale on the bulk properties of hardness of the material being machined.

3.2 Sampling Process and Parameter Estimation

As shown in Fig. 2, the geometric shape of each sample is a parallelepiped being $\pi \mathrm{D}/n_s$ long and a cross-sectional area equal to a product of depth of cut and feed. Due to the nonhomogeniety, each sample holds its distinct ratio of microstructures in it. Therefore, the mean of sample hardness or the sample hardness mean, μ_s, is different from sample to sample. The sample hardness mean μ_{sj} for the j^{th} sample can be obtained as

$$\mu_{sj} = \frac{1}{N_s} \sum_{i=1}^{N_s} H_i \tag{2}$$

where N_s = number of locations within a sample (a subset of measurement locations, n), and j = $1, 2, \cdots, n_s$

The mean hardness values of all samples $(\mu_{s1}, \mu_{s2}, \cdots, \mu_{sn_s})$ would be equal if the microstructures in the material were ideally uniformly distributed (in a micro-scale). However, this never is the case in practice. As a result, the sample hardness mean, μ_s, differs from sample to sample. In fact, this variation reveals, from a micro-base analysis, the main source of the random excitation phenomenon observed during machining. When the cutting tool is cutting a sample (a portion of the circumference of the workpiece being cut) with a small value of mean hardness, the magnitude of the cutting force drops. On the other hand, the cutting force jumps up when the cutting tool is meeting a sample with a large value of mean hardness. Because the variation in the mean hardness value from sample to sample is of random nature, the dynamic variation of the cutting force during machining is also

of random nature. The larger the mean hardness value variation, the stronger the random excitation system present during machining.

Since the sample hardness mean μ_s - the key parameter of the random excitation system, is a random variable, it is best dealt with statistically. Based on the central limit theorem in statistics, the distribution of the sample hardness mean, or the μ_s distribution, can be approximated by a normal distribution because each sample contains a large number of sample attributes. Accordingly, the two parameters $\overline{\mu_s}$ and σ_s^2 of the normal distribution representing the random excitation model can be quantitatively evaluated from the sample hardness mean values, μ_{sj} for $j = 1, 2, \cdots, n_s$.

It can be shown that the mean of the sample mean distribution is equal to the mean of its population distribution, i.e., $\overline{\mu_s} = \mu_a$. However, estimating the variance of the sample hardness mean distribution, or the sample mean variance, using the standard statistical formulas, is not practical because such an evaluation would require the subgrouping of the identified locations of microstructures into individual samples. Whenever the geometric sample shape changes, say a change of feed, a re-subgrouping process is needed to evaluate the sample mean variance under the new geometric sample shape. Therefore, this procedure to evaluate σ_s^2 would be extremely tedious if applied in practice. Furthermore, the main drawback of this procedure is that a quantitative relationship between the sample mean variance and the geometric sample shape, namely, the three cutting parameters cannot be easily established.

Estimation of the Variance of Sample Hardness Mean Distribution

The sample mean variance theory is employed to establish the quantitative relation between the sample mean variance and the geometric sample shape. The theory itself stemmed from the need to characterize the composition uniformity of a chemical mixing process, a similar process of taking random samples from the population distribution and evaluating the sample mean values afterwards. The theory offers a mathematical approach to quantitatively evaluate the sample mean variance based on the knowledge of the mean, the variance, and

the correlation coefficient function of the population distribution, from which the random samples are being taken.

According to this approach, a concept of the *geometric sample shape function* $W(r)$ is first introduced to quantitatively describe the influence of the geometric characteristics of a sample drawn from the population on the evaluation of the sample mean variance. As explained in the APPENDIX, the geometric sample shape function is defined as a volume integral, and is given as follows:

$$W(r) = \frac{1}{vol} \int_{vol} W^*(x, r) dv \tag{3}$$

where vol = sample volume.

The integrand $W^*(x, r)$ in Eq.(3) is the volume fractional function which will be equal to 1.0 if the entire area of a shell constructed at location x with a radius r lies inside the sample as illustrated in Fig. A1. On the other hand, it will be equal to zero if none of the constructed shell is contained by the sample shape. It will be in the range from 0 to 1 if only part of the constructed shell is contained by the sample shape.

By knowing the population variance σ_a^2, the correlation coefficient function $\rho(r)$, and the geometric sample shape function $W(r)$ for a given geometric sample shape, *without the subgrouping process*, the corresponding sample mean variance σ_s^2 can be predicted using the following equation (its derivation is given in APPENDIX).

$$\sigma_s^2 = \frac{4\pi\sigma_a^2}{vol} \int_{r=0}^{\infty} \rho(r) W(r) r^2 dr = 4\pi\sigma_a^2 (\frac{n_s}{f\ d\ v}) \int_{r=0}^{\infty} \rho(r) W(r) r^2 dr \tag{4}$$

Note that Eq.(4) consists of two parts. One part is the integral, $\int_{r=0}^{\infty} \rho(r) W(r) r^2 dr$, and the other is the constant term calculation, $\frac{4\pi\sigma_a^2}{vol}$, or $4\pi\sigma_a^2(\frac{n_s}{fdv})$. For a given workpiece material under different cutting parameter settings, the constant term decreases as any of the three cutting parameters increases. This is due to an increase of parameter vol appearing in the denominator which is given by $\frac{fdv}{n_s}$. The integral term always increases as any of the three cutting parameters increases because the geometric sample shape function $W(r)$

always increases (sometimes very slightly) and at the same time the correlation coefficient function $\rho(r)$ remains unchanged as long as the workpiece material is unchanged. Therefore, the magnitude of the sample mean variance σ_s^2 is a compromise between these two terms. In fact, Eq.(4) serves as a mathematical model to predict values of the sample mean variance under different cutting parameter settings.

3.3 A Model for Random Excitation System

The random excitation system can be mathematically described by a normal distribution as shown in Fig. 3. The mean level $\overline{\mu_s}$ is directly related to the mean level of the dynamic cutting force. For those samples on the left side of $\overline{\mu_s}$ shown in Fig. 3 (their mean hardness values are less than $\overline{\mu_s}$), magnitudes of the dynamic cutting force induced by those samples during machining are smaller than the mean level of the dynamic cutting force, and vice versa. Because the sample mean hardness value μ_{si} varies about $\overline{\mu_s}$ randomly, the generated dynamic cutting force also varies about the mean level of the dynamic cutting force randomly.

The variance of the normal distribution σ_s^2 represents the variation level of the dynamic cutting force about its mean level. The larger the variance σ_s^2, the more significant the μ_s variation level as well as the variation level of the dynamic cutting force. As the variance σ_s^2 decreases, the μ_s variation level decreases accordingly. When the variance σ_s^2 approaches to zero, indicating that all sample mean hardness values are equal to each other, the random excitation system diminishes. This resembles a special case of machining operation where the workpiece material has a uniform microstructural distribution, causing the generated cutting force to be at a certain constant level. Therefore, the two parameters, $\overline{\mu_s}$ and σ_s^2, of the normal distribution fully describe the characteristics of the random excitation system.

4 A Case Study

A turning operation to machine SAE 1015 low carbon steel material is studied to demonstrate the procedure of formulating the random excitation system. Basically, there are three steps to estimate $\overline{\mu_s}$ and σ_s^2 of the normal distribution.

1. Microstructural Analysis to identify the locations and hardness values of microstructures in a representative part taken from the SAE 1015 material to be machined.

2. Evaluation of the mean μ_a (deriving the estimate of parameter $\overline{\mu_s}$), the variance σ_a^2, and the correlation coefficient function of the microhardness distribution $\rho(r)$.

3. Evaluation of the sample mean variance σ_s^2.

Step 1. Modern technology of microstructural analysis makes it possible to accurately identify the locations and hardness values of microstructures in the material. In this case study, a specimen was made from the SAE 1015 material to be machined. After the surface treatments such as polishing and etching, the specimen was placed under a microscope. A computer-based system of automated measurement of fiber orientation was used to identify the locations of ferrite and pearlite structure over the chosen representative part of the specimen surface (a 3.6 x 3.75 mm^2 area). Within this area, 480 x 500 data points (240,000 data points) were collected from scanning the image under the microscope in 0.0075 mm intervals. Figure 4 shows two images produced under the microscope, before and after the digitized scanning and the contrast enhancement. The black areas represent locations of pearlite structures and the white areas represent locations of ferrite structures. Among the 240,000 data, it was found that 87,120 data represented the pearlite structure and 152,880 data represented the ferrite structure. This indicates that the pearlite structures occupied 36.3 % and the ferrite structures occupied 63.7 % of the representative part.

The microhardness values of the ferrite and pearlite structures were measured using a Vicker machine. Ten positions of typical ferrite and pearlite structures were selected on

the specimen surface. A diamond pyramid was pressed into each of them and the resulting Vicker Hardness Number (VHN) measurement was recorded. Table 1 lists the measured VHN values for the ferrite and the pearlite structures, respectively. The average values were calculated from the measured data and taken as the microhardness values of the ferrite and pearlite structures under investigation. Table 1 also lists the equivalent values in Brinell Hardness Number (BHN) for the ferrite and pearlite structures. For the pearlite structure, its microhardness value was 240 (BHN), and for the ferrite structure 61 (BHN).

Step 2. Based on Eqs.(2) and (3), the mean and variance values of the microhardness distribution of the workpiece material are calculated as $\overline{\mu_s} = 126\ BHN$ and $\sigma_a^2 = 7409\ BHN^2$.

The evaluated correlation coefficient function $\rho(r)$ is plotted in Fig. 5. The set of dot-lines is a linear approximation of the obtained correlation coefficient function, giving by

$$\rho(r) = \begin{cases} 1.00 - 0.20r & 0 \le r \le 3 \\ 0.40 - 0.05(r-3) & 4 \le r \le 8 \\ 0.15 - 0.01(r-8) & 9 \le r \le 13 \\ 0.10 - \frac{0.10}{46}(r-13) & 14 \le r \le 60 \\ 0 & 61 \le r \end{cases} \tag{5}$$

where r = distance in terms of the number of the basic interval (0.0075 mm) used in the digitizing data process.

Step 3. The calculated numerical values of the geometric sample shape function $W(r)$ as a function of the distance parameter r (multiples of the scanning interval) under different cutting parameter settings are plotted in Figures 6a, 6b, and 6c. Each corresponds to specific cutting parameter settings. The four curves in Fig. 6a represent the four geometric sample shape functions for the four feed settings while depth of cut and spindle speed (workpiece diameter = 50 mm) are fixed at 0.5 mm and 600 rpm, respectively. Table 2 provides the numerical values used for plotting the four geometric sample shape functions associated with the four feed settings. It is evident that when the cutting parameter of feed increases, this geometric sample shape function increases significantly because of a significant increase of the volume fractional function $W^*(x, r)$ in Eq. (3). On the other hand, as indicated in

Fig. 6c, the geometric sample shape function changes little as the spindle speed increases. In fact, there appears to be only a single curve because the change of this function is so small that the existing differences among the four geometric sample shape functions under the four different spindle speeds can hardly be displayed by the current scale used in Fig. 6c.

Knowing $\sigma_a^2, \rho(r)$, and $W(r)$, the sample mean variance σ_s^2 are evaluated based on Eq.(4). Figure 7 presents the evaluated sample mean variance σ_s^2 as a function of feed, depth of cut, and spindle speed, respectively. The curve with the slowest decaying rate represents the sample mean variance σ_s^2 under different feed settings while depth of cut and spindle speed are fixed at 0.5 mm and 600 rpm, respectively. The increase of feed has two effects on the evaluation of the sample mean variance σ_s^2. The first effect is to increase the sample volume, as illustrated in Fig. 2. A large sample volume usually averages out the influence due to the nonhomogeneous distribution of microstructures. The second effect is to increase the dimension of sample related to feed, as illustrated in Fig. A1. As this dimensional size approaches the dimensional size related to depth of cut, the volume fractional function $W^*(x, r)$ increases. The combination of these two effects gives rise to the slow decaying rate of the sample mean variance σ_s^2 as feed increases, especially in a small feed range. This fact is also evidenced by examining Eq. (4). The decrease in the constant term as feed increases is somehow balanced by an increase in the integral term. This result suggests that under small feeds, the random excitation system plays an important role in the determination of tool random vibratory motion during machining. The curve with the fastest decaying rate in Fig. 7 represents the sample mean variance σ_s^2 under different spindle speed settings while depth of cut and feed are fixed at 0.5 mm and 0.10 mm/rev, respectively. Increasing the spindle speed setting has the same effect on the sample volume as does increasing the feed setting. However, it has the least effect on the evaluation of the volume fractional function $W^*(x, r)$ because the dimension of sample related to cutting speed is usually the largest among the three dimensions. Thus, the decrease in the constant term in Eq.(4) dominates the evaluation of the sample mean variance σ_s^2, showing a rapidly decaying rate in Fig. 7.

This further implies that the variation level of the random excitation system decays quickly as cutting speed increases.

In Fig. 7, the ratio of $\frac{\sigma_s^2}{\sigma_a^2}$, which is the normalized sample mean variance, is also listed and labeled. This ratio has been given a special technical name *intensity of segregation*. It is a quantitative index describing the degree of segregation under a given cutting parameter setting. The intensity of segregation would have a value of zero when the microstructural characteristics of each sample assumed to be taken along the circumference of the workpiece has no significant difference from the statistical point of view. As indicated in Fig. 7, the intensity of segregation is relatively strong (0.0231 - 0.0238) when the selected feed is small (0.10 mm/rev to 0.20 mm/rev) indicating that the random excitation system is rather powerful for this case. It weakens when the selected feed reaches to a value of about 0.35 mm/rev.

5 Experimental Work

Boring machining tests were carried out as shown in Fig. 8. The workpiece material was low carbon steel SAE 1015. To facilitate the profile measurements, the outer surface instead of the inner surface was machined. Roughness profiles of the machined surfaces were traced by a TALYSURF-10 profilometer. Skidless measurements were taken to eliminate the influence of such factors as cut-off and skid in the assessment of average roughness R_a.

Table 3 lists, in the first row, the measured R_a values of the machined surfaces under the cutting conditions where only the cutting parameter of feed varied (depth of cut = 0.50 mm and spindle speed = 600 rpm). Each of the measured R_a values is decomposed into deterministic and stochastic portions. The numerical values of the deterministic portion, listed in the second row, were calculated based on the geometry and the formula proposed by Boothroyd [6]

$$R_a = \frac{0.0321 f^2}{R} 10^3 \quad (\mu m) \tag{6}$$

where f = feed (mm/rev) and R = tool nose radius (mm).

The difference between the measured R_a value and its theoretical R_a value for a specific cutting parameter setting is assumed to represent the part of the profile height variation contributed by the random excitation during machining. This difference is listed in the third row marked as a *Random* R_a value. The three curves in Fig. 9 represent the data in the three rows, respectively. The solid curve representing the *Random* R_a value decreases as the feed increases. This decreasing pattern is very similar to the curve pattern shown in Fig. 7 where the sample mean variance σ_s^2 decreases as feed increases. This similarity confirms the validity of using the sample mean variance as an index to quantitatively represent the existence of a random excitation system present during machining. As illustrated in Fig. 9, the measured R_a value, when f = 0.25 mm/rev was used, is closer to the theoretical R_a curve than others. This indicates that a good prediction of the R_a value of a machined surface based on Eq.(6), can be made only when the selected feed is relatively large. When the selected feed is relatively small, the *random* R_a value is usually, as indicated in Fig. 7, twice or three times as high as the predicted R_a value. Under such circumstances, the prediction based on Eq. (6) is meaningless due to the additional surface irregularities introduced by a rather powerful random excitation system present during machining.

The present approach may also shed some light on the results of Miller, et al. [8], who observed the poor prediction of the R_a values at a low spindle speed. Figure 10 shows the contour plot of constant R_a values. The dashed line marked as 3.8 μm represents the calculated R_a value from Eq.(6). The curve in solid line also marked as 3.8 μm represents the contour associated with the measured R_a values equal to 3.8 μm. Two lines with arrows on them show the distance between the prediction line from Eq. (6) and the 3.8 μm - contour under different cutting conditions. This distance decreases as cutting speed increases because the strength of the random excitation system decreases as cutting speed increases. However, this distance never disappears, or the theoretical prediction line always serves as an asymptote due to the presence of the random excitation system, a physical phenomenon which is unavoidable. This points out the limitation on achievable surface

finishing quality regarding the surface irregularities produced during machining. Control of the microstructural characteristics of part material plays an important role in this regard.

6 Conclusions

1. A statistical approach is employed to study the mechanism of random excitation phenomena observed during machining. The nonhomogeneous distribution of microhardness present in the material has been considered a major random excitation source which affects the formation of surface irregularities. A normal distribution model is used to represent the random excitation system with mean and variance as its two parameters characterizing the average and variation levels of the random excitation system.

2. A procedure has been developed to compute the two model parameters in terms of the the three cutting parameters, the correlation coefficient function, and the geometric sample shape function. The correlation coefficient function characterizes the size, shape, and segregation of the microstructure. The geometric sample shape function directly relates the cutting geometry to the microstructure distribution. These two functions make possible a quantitative representation of the random excitation system present during machining.

3. Results of the theoretical relationship between the strength of the random excitation system in terms of the sample variance and the three cutting parameters of depth of cut, feed, and spindle speed (or cutting speed) has been verified through surface roughness measurements. At low values of feed and cutting speed, the effect of random excitation is more significant than the effect at higher values of feed and cutting speed. These findings are in agreement with the theoretical results.

In summary, the present research has provided an insight about how the basic characteristics of the microstructures of the part material being cut relate to the dynamic generation

of surface irregularities during machining. A procedure will be developed in Part 2 of this paper to construct the texture of machined surfaces with both the deterministic component caused by the tool geometrical motion and the stochastic component due to tool random vibration based on the model developed in this paper.

Acknowledgments

The authors acknowledge the support of the Systems Research Center at the University of Maryland at College Park under Engineering Research Centers Program: NSFD CDF 8803012, and the support of the University of Illinois Office of Advanced Engineering Studies Research Program. They also express gratitude to Dr. C. L. Tucker for indicating the usefulness of the sample variance theory in this work, and to Mr. M. Lovrich for conducting the microstructural analysis.

References

1. T. Sata, 'Surface Finish in Metal Cutting,' *Annals of the CIRP*, Vol. 12, 1963, pp. 190-197.

2. J. Peklenik, 'Investigation of the Surface Typology,' *Annals of the CIRP*, Vol. 15, 1967, pp. 381-385.

3. R. E. DeVor and S. M. Wu, 'Surface Profile Characterization by Autoregressive Moving Average Models," *ASME Trans.*, Series B, Vol. 94, No. 3, 1972, pp. 825-832.

4. D. J. Whitehouse, P. Vanherck, W. deBruin, C. A. vanLuttervelt, 'Assessment of Surface Typology Analysis Techniques in Turning,' *Annals of the CIRP*, Vol. 32/2, 1974, pp. 265-282.

5. A. Villa, S. Rossetto, and R. Levi, 'Surface Texture and Machining Conditions, Part 1: Model Building Logic in View of Process Control,' *ASME Trans.*, Series B, Vol. 105, No. 4, 1983, pp. 259-263.

6. G. Boothroyd, 'Fundamentals of Metal Machining and Machine Tool,' Scripta Book Co., 1975.

7. S. M. Pandit and S. Revach, 'A Data Dependent System Approach to Dynamics of Surface Generation in Turning," *Journal of Engineering for Industry*, ASME Trans., Vol. 103b, 1981, pp. 437-445.

8. J. C. Miller, J. W. Sutherland, and R. E. DeVor, 'Surface Roughness Characteristics for Turning 380 and 390 Aluminum Casting Alloys,' *Proceedings of 10th North American Manufacturing Research Conference*, May 1982, pp. 282-288.

9. P. V. Danckwerts, 'The Definition and Measurement of Some Characteristics of Mixtures,' *Applied Scientific Research*, A3, 1952, pp. 279-296.

10. C. J. Tucker III, 'Sample Variance Measurement of Mixing,' *Chemical Engineering Science*, Vol. 36, No. 11, 1981, pp. 1829-1839.

11. M. E. Merchant, 'Mechanics of the Metal Cutting Process (II) Plasticity Conditions in Orthogonal Cutting," *Journal of Applied Physics*, Vol. 16, No. 6, June 1945, pp. 318-324.

12. L. VanVlack, 'Elements of Materials Science and Engineering,' Addison Wesley, Fourth Edition, 1980, p. 36.

13. M. Kronenberg, 'Machining Science and Application,' Pergamon Press Inc., 1966, pp. 209-225.

14. G. M. Zhang and S. G. Kapoor, 'Dynamic Modeling and Analysis of the Boring Machining System,' Journal of Engineering for Industry, Transactions of the ASME, Vol. 109, August 1987, pp. 219-226.

Appendix

Derivation of the Sample Mean Variance σ_s^2 Estimation

Consider a mixture of two substances, A and B . Let their concentrations at the i^{th} point be H_i and G_i. The mean and variance of the concentration of substance A in the mixture with total volume TV can be found as

$$\mu_a = \frac{1}{TV}\int_{TV} H_i dv \tag{A 1}$$

$$\sigma_a^2 = E[(H_i - \mu_a)^2] \tag{A 2}$$

If samples with identical geometric shape and size are taken from the mixture, the average concentration of substance A in an individual sample is given by

$$\mu_s = \frac{1}{vol}\int_{vol} H_i dv \tag{A 3}$$

where H_i = concentration of substance A at point i, and

vol = volume of the sample taken.

The sample mean μ_s is a random variable. Based on the central limit theorem in statistics, its distribution is of the normal nature. The mean and variance of this normal distribution are given by

$$\overline{\mu_s} = E[\mu_s] = \mu_a \tag{A 4}$$

$$\sigma_s^2 = E[(\mu_{sj} - \mu_a)^2] = E[\frac{1}{vol^2}\int_{vol}\int_{vol}(\mu_{sk} - \mu_a)(\mu_{sl} - \mu_a)dv'dv] \tag{A 5}$$

If the number of identically shaped samples taken from the mixture is M, the expectation sign in Eq.(A5) can be replaced by a summation sign.

$$\sigma_s^2 = \frac{1}{M}\sum^{M}\frac{1}{vol^2}\int_{vol}\int_{vol}(\mu_{sk} - \mu_a)(\mu_{sl} - \mu_a)dv'dv \tag{A 6}$$

Introducing the correlation coefficient function $\rho(r)$, Eq.(A6) can be simplified as

$$\sigma_s^2 = \frac{\sigma_a^2}{vol^2}\int_{vol}\int_{vol}\rho(r)dv'dv \tag{A 7}$$

By defining a spherical shell of radius r with a thickness dr, and centered at location k (Fig. A1), the inner integral in Eq.(A7) can be written as

$$\int_{vol} \rho(r) dv' = \int_{r=0}^{\infty} \rho(r) W^*(x,r) 4\pi r^2 dr \qquad \text{(A 8)}$$

where $W^*(x,r)$ is the volume fractional function. The numerical range of this function is between zero and unity. Substituting Eq.(A8) in Eq.(A7) derives the following.

$$\sigma_s^2 = \frac{4\pi\sigma_a^2}{vol} \int_{r=0}^{\infty} \rho(r) r^2 [\frac{1}{vol} \int_{vol} W^*(x,r) dv] dr \qquad \text{(A 9)}$$

The terms within the square brackets in Eq.(A9) are related to the sample geometry only. Define this part as the sample shape function $W(x,r)$ because it can be integrated with respect to the sample volume separately.

$$W(x,r) = \frac{1}{vol} \int_{vol} W^*(x,r) dv \qquad \text{(A 10)}$$

By substituting Eq.(A10) into Eq.(A9), the formula to evaluate the sample mean variance is given by, which is the same formula as Eq.(4) in the text.

$$\sigma_s^2 = \frac{4\pi\sigma_a^2}{vol} \int_{r=0}^{\infty} \rho(r) W(r) r^2 dr = 4\pi\sigma_a^2 (\frac{n_s}{f\ d\ v}) \int_{r=0}^{\infty} \rho(r) W(r) r^2 dr \qquad \text{(A 11)}$$

Table 1: Measured Microhardness Values of Ferrite and Pearlite Structures
(Loading: 100 kgs and Diamond Pyramid: 136 degrees)

Location No.	Ferrite	Pearlite
1	66.3	254
2	67.0	243
3	66.5	249
4	68.6	238
5	67.0	251
6	67.8	240
7	66.5	253
8	68.0	247
9	67.5	243
10	66.8	246
Average in VHN	67.2	246
Equivalent in BHN	61.0	240

Table 2: Calculated $W(x, r)$ Values for the Four Different Feed Settings

Distance r x 0.0075 mm	Feed (mm/rev) 0.10	0.20	0.30	0.40
0	1.00	1.00	1.00	1.00
1	0.91	0.94	0.96	0.96
2	0.87	0.92	0.94	0.94
3	0.83	0.90	0.91	0.93
4	0.78	0.86	0.89	0.91
5	0.75	0.84	0.87	0.90
6	0.71	0.81	0.86	0.87
8	0.65	0.77	0.82	0.84
10	0.58	0.73	0.78	0.81
14	0.45	0.65	0.71	0.75
18	0.31	0.57	0.66	0.70
25	0.18	0.41	0.53	0.61
30	0.12	0.32	0.46	0.53
40	0.07	0.17	0.30	0.36
50	0.05	0.11	0.20	0.27
60	0.04	0.08	0.14	0.22

Table 3: Measured R_a Values and their Decompositions

Feed Settings (mm/rev)	0.10	0.15	0.20	0.25
Measured R_a (μm)	2.30	2.80	2.85	3.15
Theoretical R_a (μm)	0.40	0.90	1.61	2.51
Random R_a (μm)	1.90	1.70	1.24	0.64

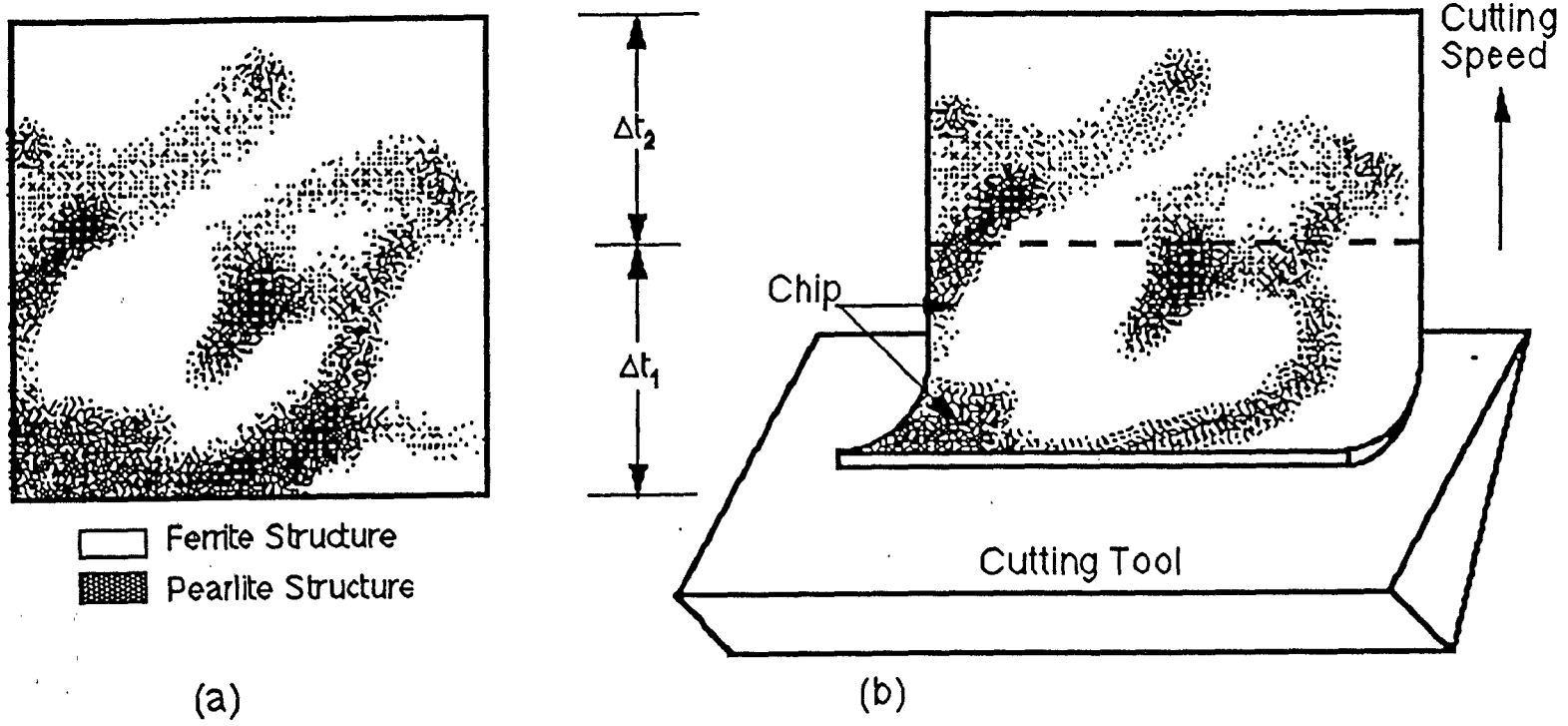

Fig. 1 A Micrograph Showing Microstructure Distribution in Mild Carbon Steel

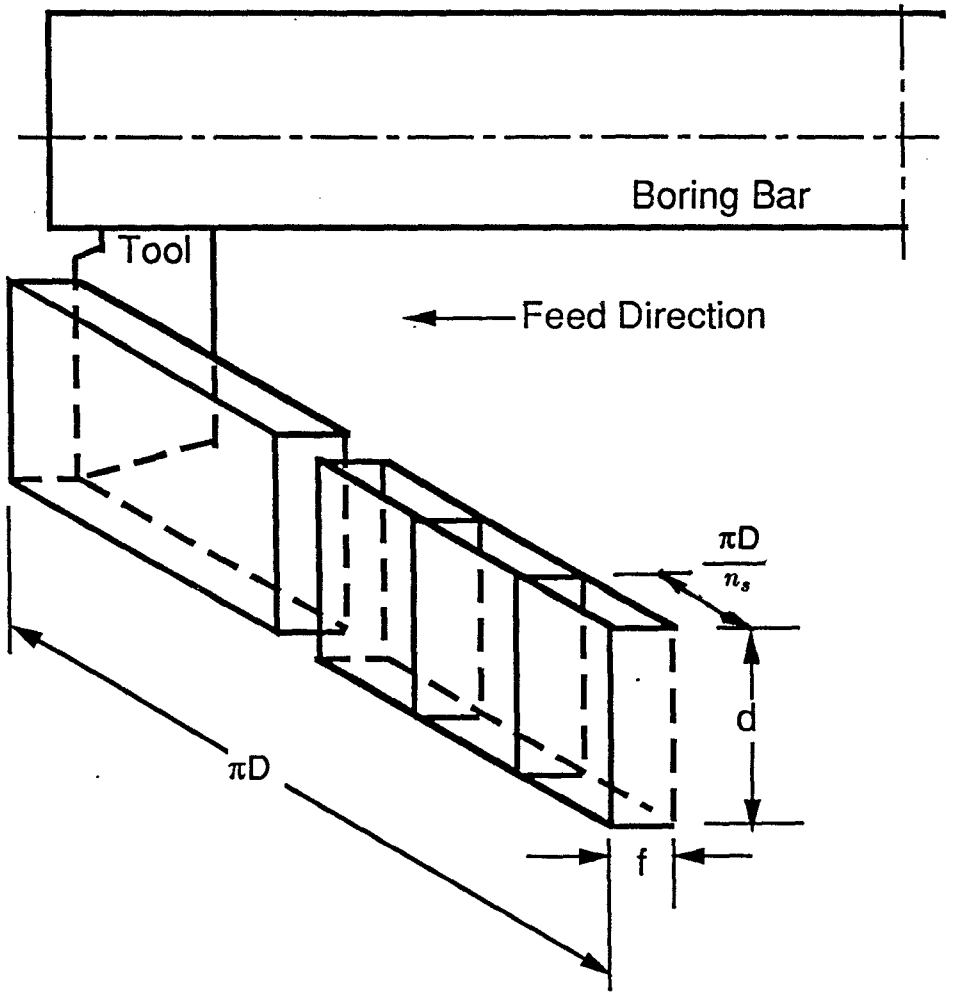

Fig. 2 Geometric Shape and Size of Samples Assumed During Machining

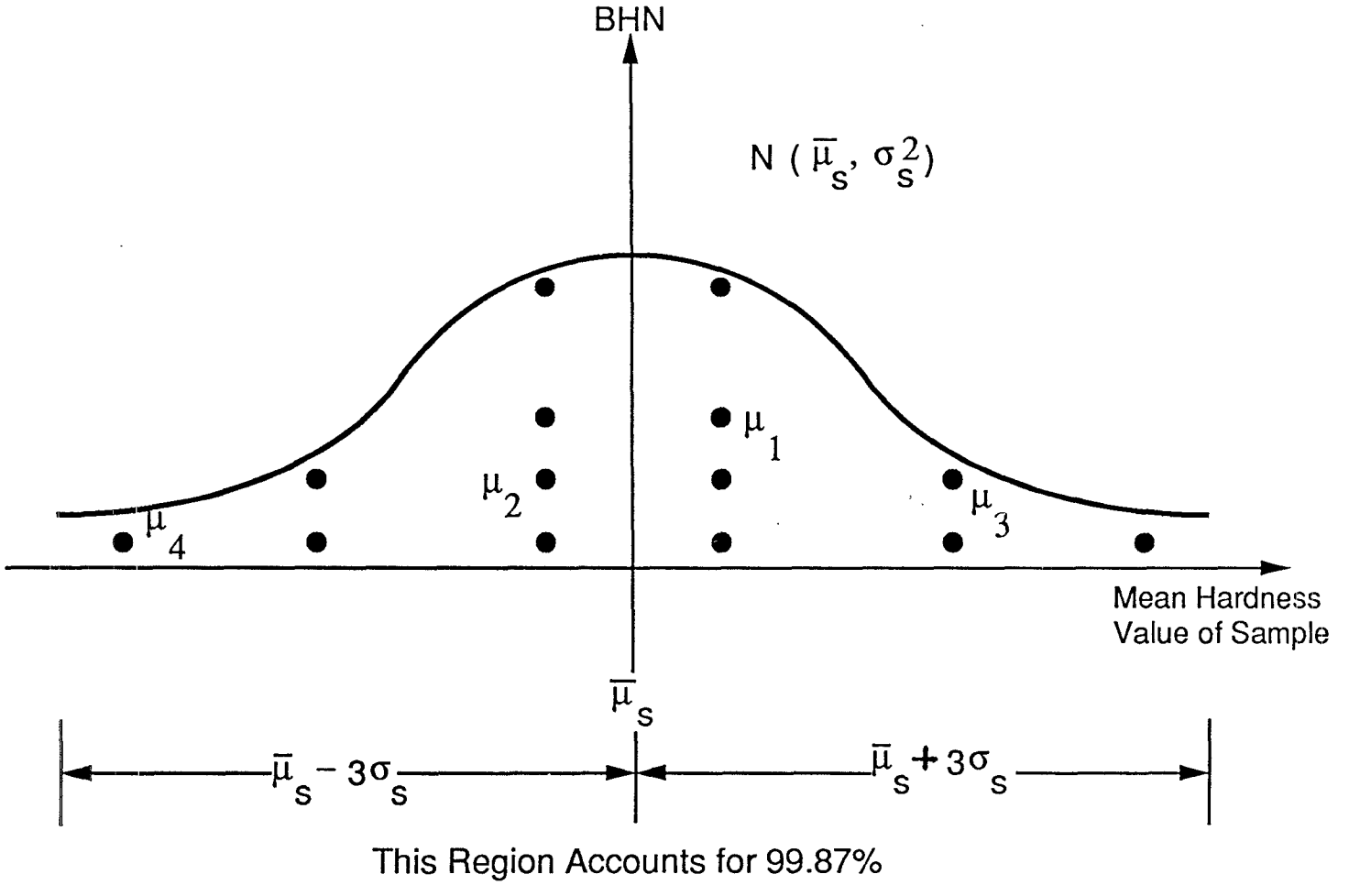

Fig. 3 Normal Distribution Model of the Random Excitation System

(a) After Digitation and Before Contrast Enhancement

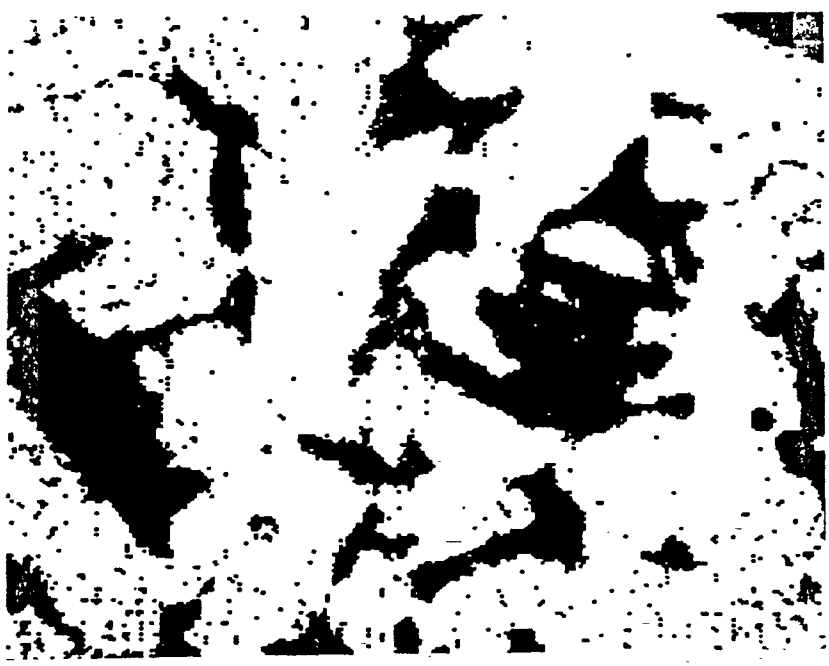

(b) After Contrast Enhancement

Fig. 4 Sample Images before and after Contrast Enhancement

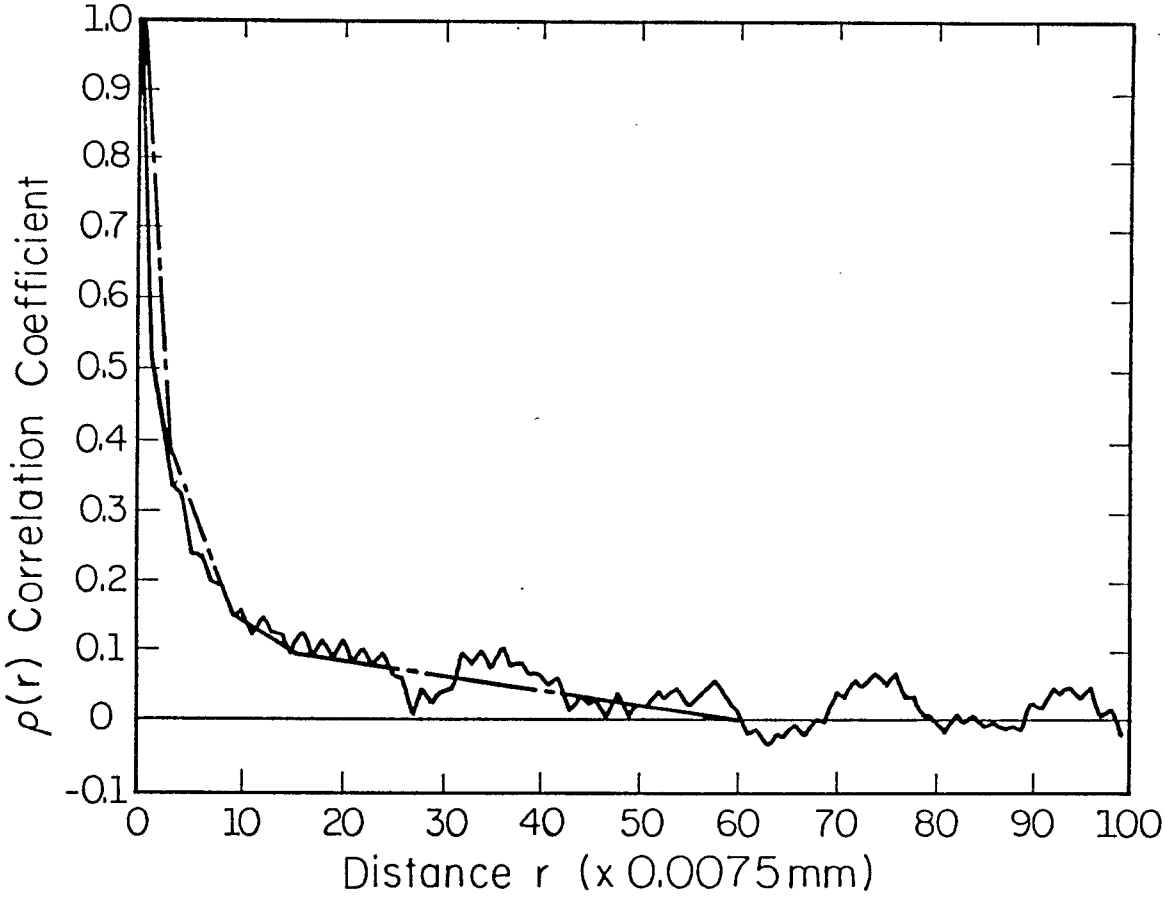

Fig. 5 Correlation Coefficient Function and its Approximate Form

(a)

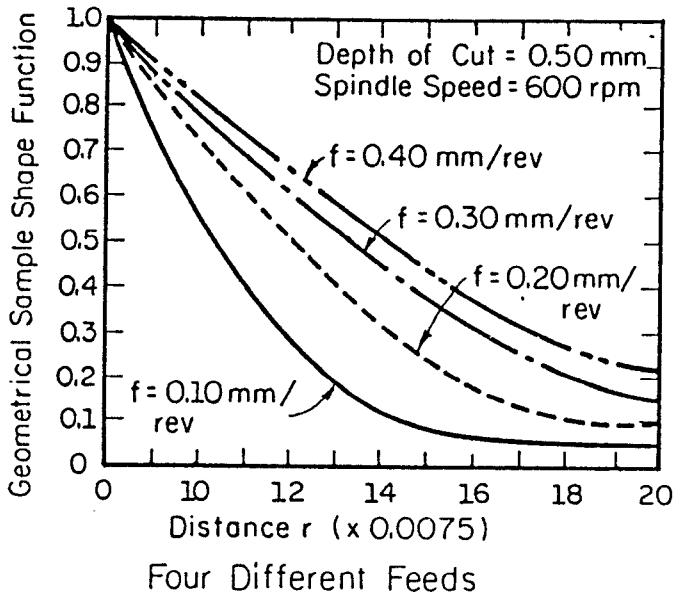

Four Different Feeds

(b)

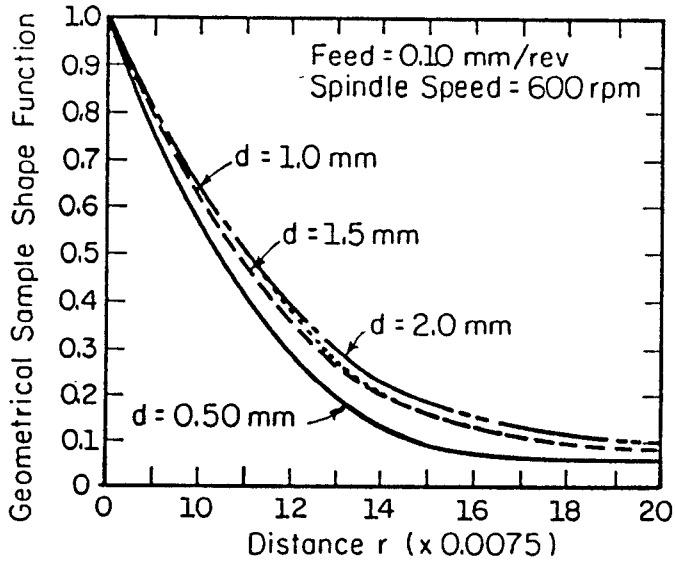

Four Different Depth of Cuts

(c)

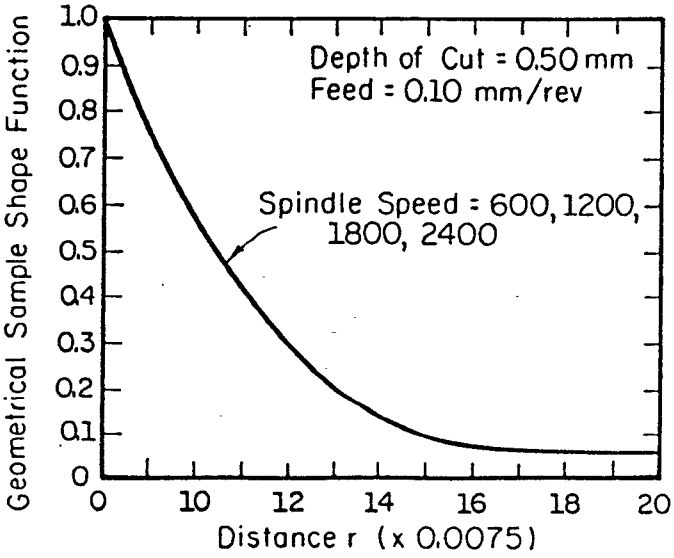

Fig. 6 Plot of Geometric Sample Shape Function

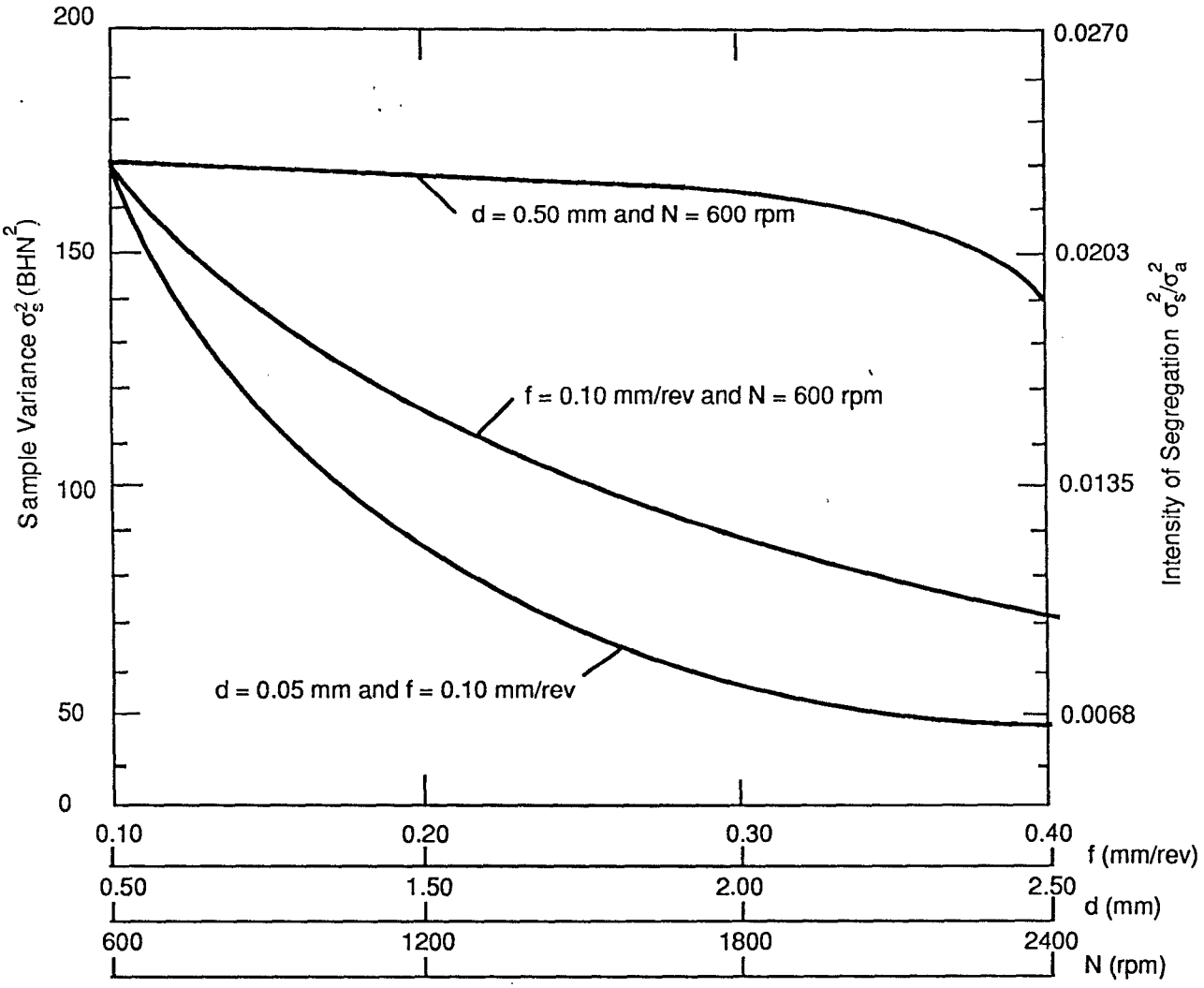

Fig. 7 Plot of Sample Variance Estimation

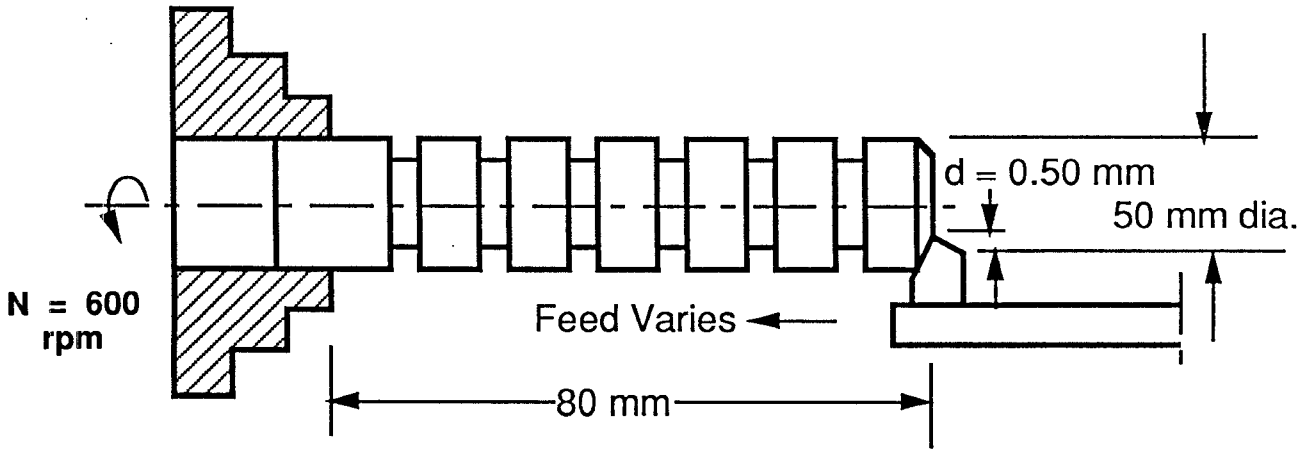

Fig. 8 Experimental Setup for Boring Machining Tests

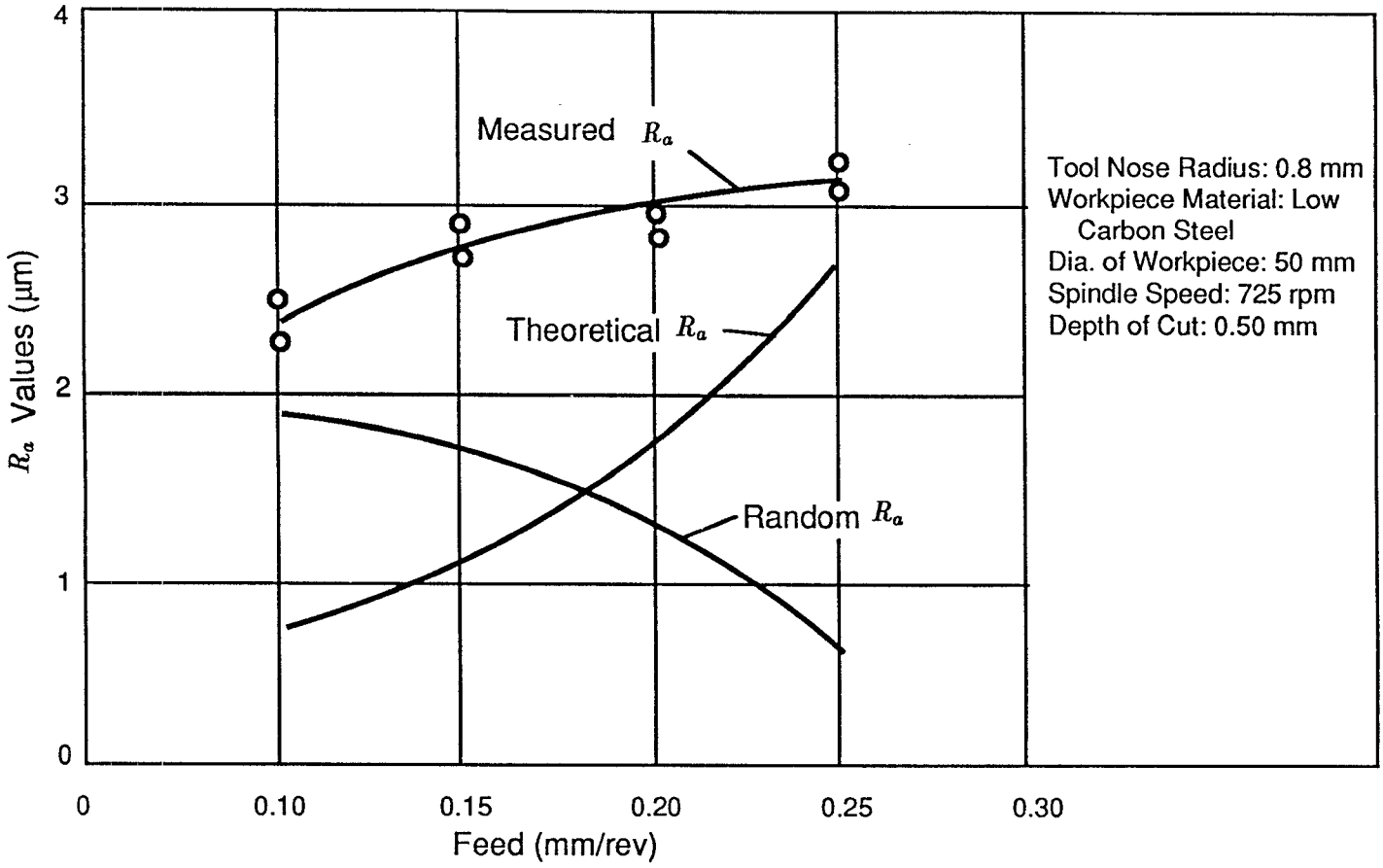

Fig. 9 Decomposition of Surface Roughness Index R_a value

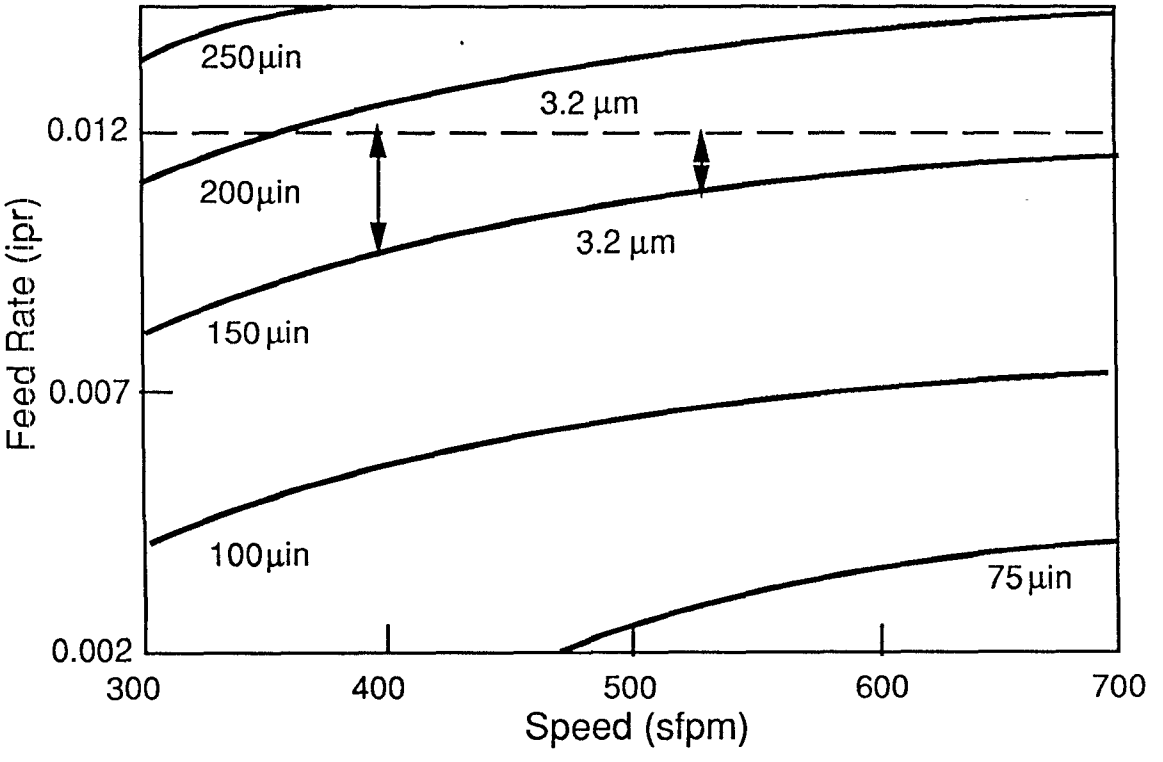

Fig. 10 Experimental Results Provided by Miller [7]

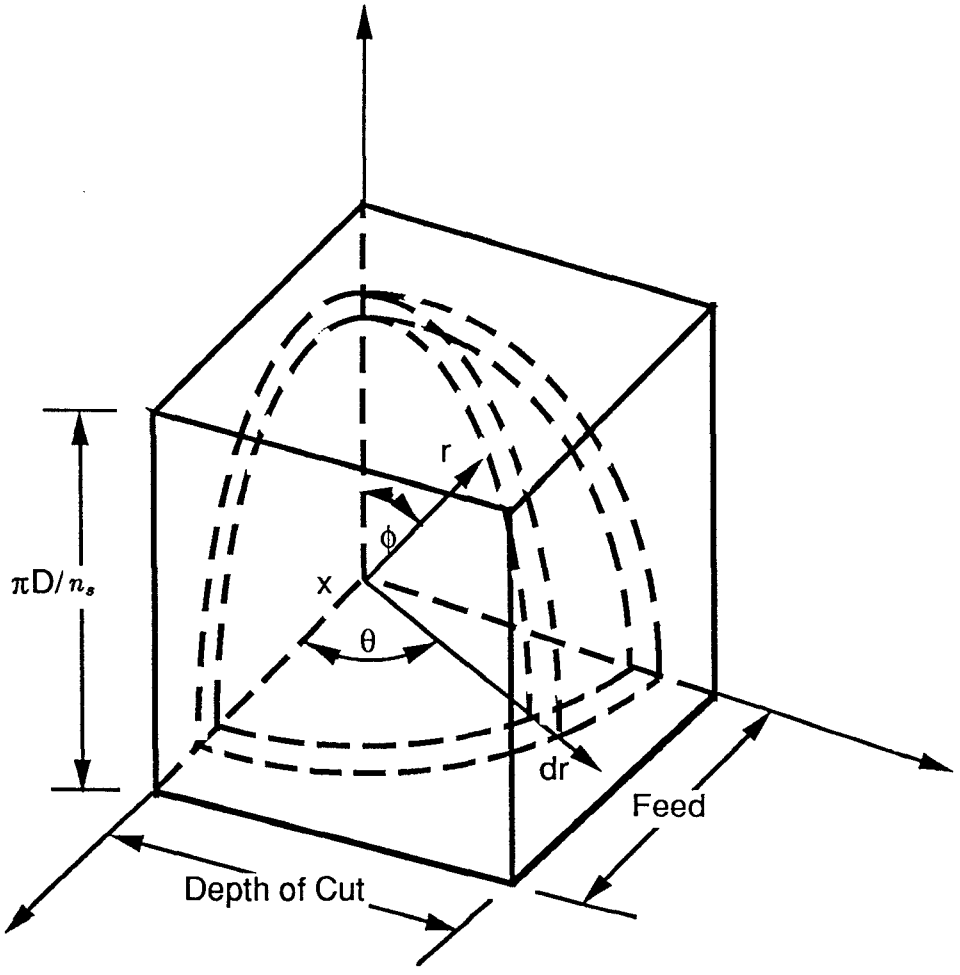

$$W^*(x,r) = \frac{\text{Volume of the shell lying inside the sample}}{\frac{4\pi}{3}\left[(r+dr)^3 - r^3\right]}$$

Fig. A1 Definition of the Volume Fraction Function $W^*(x,r)$

NOMENCLATURE

R_a = surface roughness index, μm

BHN = Brinell hardness number

D = diameter of the workpiece being machined, mm

d = depth of cut, mm

f = feed, mm/rev

f_{max} = highest cutting force frequency component of interest

H_i = microhardness value at the i^{th} location

i = index for the order of locations within the sample

j = index for the order of samples taken along the circumference

n = number of locations taken on the chosen representative part

N_s = number of locations taken within a sample

n_s = number of samples taken along the circumference per one revolution

r = distance in terms of the number of the basic interval used in digitizing

N = spindle speed, rpm

T = machining time during one revolution of workpiece, sec

VHN = Vicker hardness number

v = cutting speed, m/min

vol = sample volume

$W(r)$ = geometric sample shape function

$W^*(x,r)$ = volume fractional function

μ_a = mean of the population distribution of hardness,
or mean of the sample hardness means, BHN

μ_s = sample hardness mean, BHN

$\overline{\mu_s}$ = mean of the sample hardness means, BHN

σ_s^2 = variance of the sample hardness means, BHN^2

Δt_1 = machining time needed to cut the lower part, sec

Δt_2 = machining time needed to cut the upper part, sec

$\rho(r)$ = correlation coefficient function of the microhardness distribution